MS-No.: os-2020-33

Version: Revision

Title: Subsurface Initiation of Deep Convection near Maud Rise

Author(s): René M. van Westen and Henk A. Dijkstra

Point-by-point reply to reviewer #2

September 24, 2020

We thank the reviewer for his/her careful reading and for the useful comments on the manuscript. Below is a point-by-point reply with references to figures which are placed at the bottom of the document.

Specific Comments:

1. *The growing subsurface instabilities that precede the polynya in CESM model year 231 (Fig. 3a, 3b) are intriguing. It would be great if the authors could discuss in further detail what mechanism is behind the growing instability. Is it related to the multidecadal buildup of subsurface heat, mentioned in pg. 12, L24-25? Or is a shorter-timescale process more relevant here? Pg. 8 would be a good place to discuss this.*

   Author's reply:
   We have conducted additional analysis on the Weddell Deep Water (WDW), see Figure 1). During Maud Rise Polynya (MRP) events, the WDW temperature decreases as heat is ventilated by vertical mixing. After the MRP event during model years 205 – 209, the WDW is relatively cold and the temperature increases over time. Prior to model year 231, the WDW temperature reaches maximum values which corresponds to the growing subsurface static instabilities. In model year 231, an MRP forms and the WDW temperature decreases again. The build-up of the WDW heat reservoir has the same dominant period of the multidecadal build-up of subsurface heat over Maud Rise.

   Changes in manuscript:
   We will include an analysis of the properties of the WDW in the revised manuscript. Here we will discuss the multidecadal build-up of subsurface heat is causing the growing subsurface static instabilities.

2. *The aforementioned subsurface instabilities also appear to occur in the model years preceding year 231 (Fig. 3c). If these instabilities play a role in initiating convection, why are there no polynyas during this previous time period? Are unfavorable near-surface conditions inhibiting deep convection from above? The time series of wind stress curl, as shown in Fig. 3a, could be useful if it is extended to include this earlier time period.*

   Author's reply:

   We have analysed the daily-averaged and monthly-averaged wind-stress curl fields for model years 229, 230 and 231 averaged over the Polynya region. In addition, we determined the wind-stress curl climatology (model years 150 – 250). The climatology shows a persistent negative wind-stress curl over all the months, as well as during model years 229, 230 and 231 (Figure 2a).

   We find that during model year 229, the monthly-averaged wind-stress curl is weaker (less negative) w.r.t. climatology during August and October; for September it is slightly stronger (more negative) w.r.t. the climatology mean. For model year 230, the wind-stress curl is weaker w.r.t. the climatology mean during August – October. For August model year 231 (during this month an MRP formed), the wind-stress curl is stronger w.r.t. the climatology mean. On the other hand, while analysing daily-averaged fields (Figure 2b), we find strong negative values for the wind-stress curl during model years 229, 230 and 231. These strong negative values are associated with the passing of (strong) winter cyclones.

   Another important effect of MRP formation is the magnitude of the subsurface static instabilities (Figure 3a). There are indeed subsurface instabilities during model years 229 and 230, as pointed out by the reviewer. However, the magnitude of these static instabilities is much smaller compared to the ones in model year 231. For example, when taking the depth-averaged and monthly-averaged static instabilities between 200 – 1000 m depths (Figure 3b), the subsurface static instabilities are a factor 4.8 (August model year 229) and 7.9 (August model year 230) smaller compared to August model year 231. Even with favourable near-surface conditions, such as strong winter cyclones, the subsurface static instabilities are not strong enough to cause convection in the years before model year 231.

Changes in manuscript:
We will include the climatology of the wind-stress curl and the monthly-averaged and daily-averaged results in the revised manuscript. We will discuss why an MRP did not form in the years prior to model year 231, making use of the monthly-averaged and depth-averaged static instabilities. As mentioned in the manuscript, due the time averaging, the magnitude of monthly-averaged subsurface static instabilities are smaller compared to daily-averaged subsurface static instabilities. To demonstrate the growing subsurface static instabilities prior to MRP formation, we will include a time series of the depth-averaged and daily-averaged subsurface static instabilities for model year 231.

3. *Pg. 8, L28-29 and pg. 9, L1-2: Wind stress curl is associated with upwelling, turbulent mixing, and sea-ice divergences. The manuscript would benefit from the authors explicitly quantifying the upwelling magnitude associated with wind stress curl anomalies. For instance, the horizontal and/or vertical Ekman velocities can be inferred from wind stress curl (e.g. Campbell et al., 2019, Methods, salinity fluxes from upwelling). This quantity could help contextualize the near-surface destratification shown in Fig. 3.*

Author's reply:
We followed the suggestion of the reviewer and determined the salt transport induced by upwelling over the Polynya region, following Campbell et al. (2019). The negative wind-stress curl (cf. Comment 2) entrains salt from below the mixed layer throughout the year. Note that we only determined the salt from upwelling during the sea-ice free months (January – May), the surface drag decreases in the presence of sea ice. The total salinity entrained by Ekman dynamics during the sea-ice free months is 0.065 Psu (time mean model years 150 – 250). For model year 229, 230 and 231 the total salinity (during sea-ice free months) is 0.139, 0.052 and 0.104 Psu, respectively (Figure 2d).

We also determined the salt averaged over the mixed layer depth (S_{ml}, Figure 2c). The S_{ml} is seasonally varying with a peak-to-peak difference of about 0.6 Psu. We determined the climatology of S_{ml} over all non-polynya years (note that vertical mixing brings up salt and skews the distribution). The S_{ml} is increasing between model years 229 –

231. However, the salinity anomalies are not anomalously high and are still within the S_{ml} climatology ($\overline{S_{ml}} = 34.42 - 34.50$ Psu, $5 - 95\%$ percentile). The S_{ml} anomaly (w.r.t. climatology mean) in August model year 231 is 0.07 Psu, the anomaly of salt entrainment by Ekman dynamics is 0.039 Psu.

The salt anomalies could in principle induce convection by surface static instabilities. Therefore, we re-run model year 231 and written out the daily-averaged vertical diffusivities (Figure 4c). We find no increase in the near-surface vertical diffusivity prior to polynya formation, however, the subsurface vertical diffusivity is strongly increasing prior to polynya formation (Figure 4d). Ekman upwelling favours the destratification of the Polynya region, but the induced salt anomalies are simply too weak to induce surface convection in model year 231.

Changes in manuscript:
We will include the analysis of Ekman upwelling and discuss the effect of salt anomalies on the destratification over the Polynya region. We will also include the results of the vertical diffusivity demonstrating that the subsurface is responsible for the overturning of the water column in model year 231.

4. *When comparing subsurface convection in CESM and Mercator output (Pg. 11, L29-35), it is important to acknowledge the magnitude of ocean heat content variability in the models used. Climate models are known to be prone to excessive subsurface heat accumulation, which has been attributed to freshwater forcing biases (Stössel et al., 2015) and weak parameterized mixing under sea ice (Heuzé et al., 2013). For instance, are subsurface warming trends between the simulated polynya events in CESM (Pg. 2, L24-25) consistent with the observed .032 K/decade trend in Weddell Deep Water temperature between 1977-2001 (Smedsrud, 2005)? What about the Mercator output? If not, the model-to-observation comparison could still be useful, but the difference must be acknowledged to properly inform the interpretation of the data.*

   Author's reply:
   We have determined the WDW properties as suggested by the reviewer (Figure 1). There is no excessive subsurface heat accumulation as reported in other studies. Between polynya years (model years 210 – 230), we find a WDW temperature trend of 0.064 K per decade. Between

model years 210 – 240, we find a trend of 0.024 K per decade. These trends are in the same order of Smedsrud (2005). The peak-to-peak difference in the WDW temperature is $\sim 0.1°C$.

The WDW temperature and salinity values are slightly higher compared to observations by about 0.1°C and 0.05 Psu. Note that the CESM had a spin-up period of 150 years. Analysing model years 1 – 10 showed that the WDW (as well as for the WSDW and WSBW) is much better in agreement with observations along the Greenwich meridian.

For the Mercator we also analysed the WDW properties between 1993 – 2018. We find relatively low WDW temperatures after several (small) polynya events, such as in 1996, 2006 and 2018, in agreement with the results presented in Campbell et al. (2019). The peak-to-peak difference in the WDW temperature is about 0.05°C, half of that compared to the CESM. The limited subsurface heat reservoir explains why subsurface convection ceases during 2016.

Changes in manuscript:
We will include an analysis of the properties (e.g. temperature and salt) of the WDW and discuss the relevant trends of these properties in the revised paper. We will also include a comparison with observational results of the WDW. Finally, the Mercator analysis will be discussed in the revision.

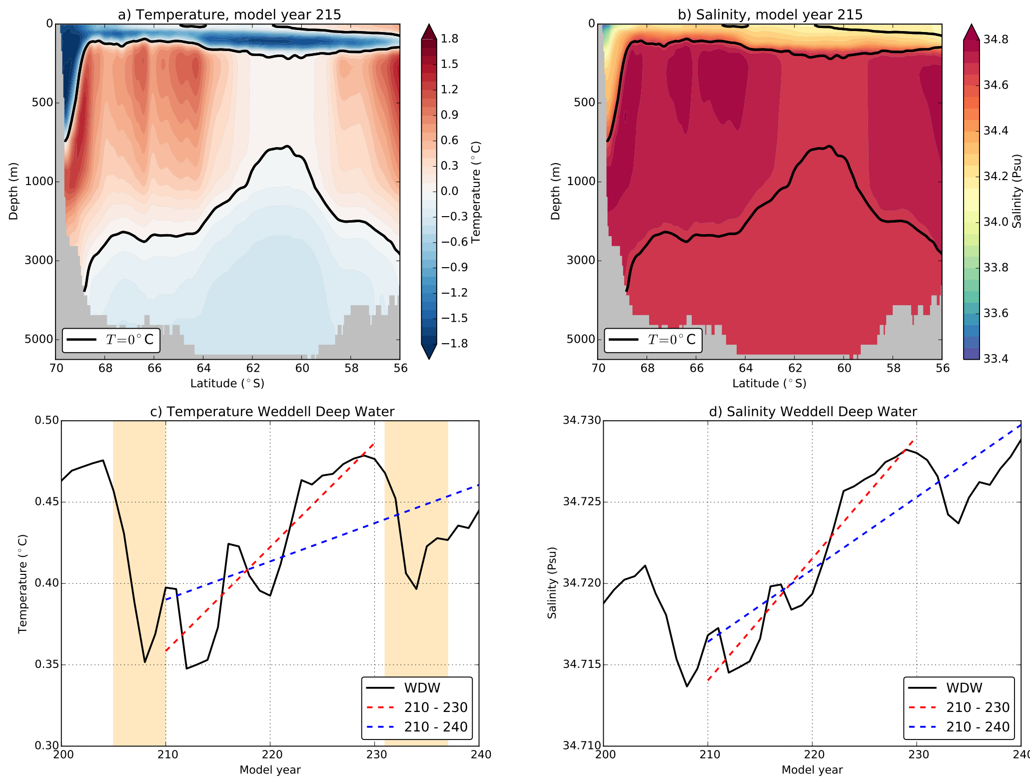

Figure 1: (a & b): Zonal mean (1°W – 1°E) of temperature and salinity along the Greenwich Meridian. The displayed values are yearly averages for model year 215. The black contour displays the 0°C, which marks the WDW. (c & d): Time evolution of the temperature and salinity of the WDW. The dashed lines are linear trends between model years 210 – 230 (red) and model years 210 – 240 (blue). The shading indicates the polynya years.

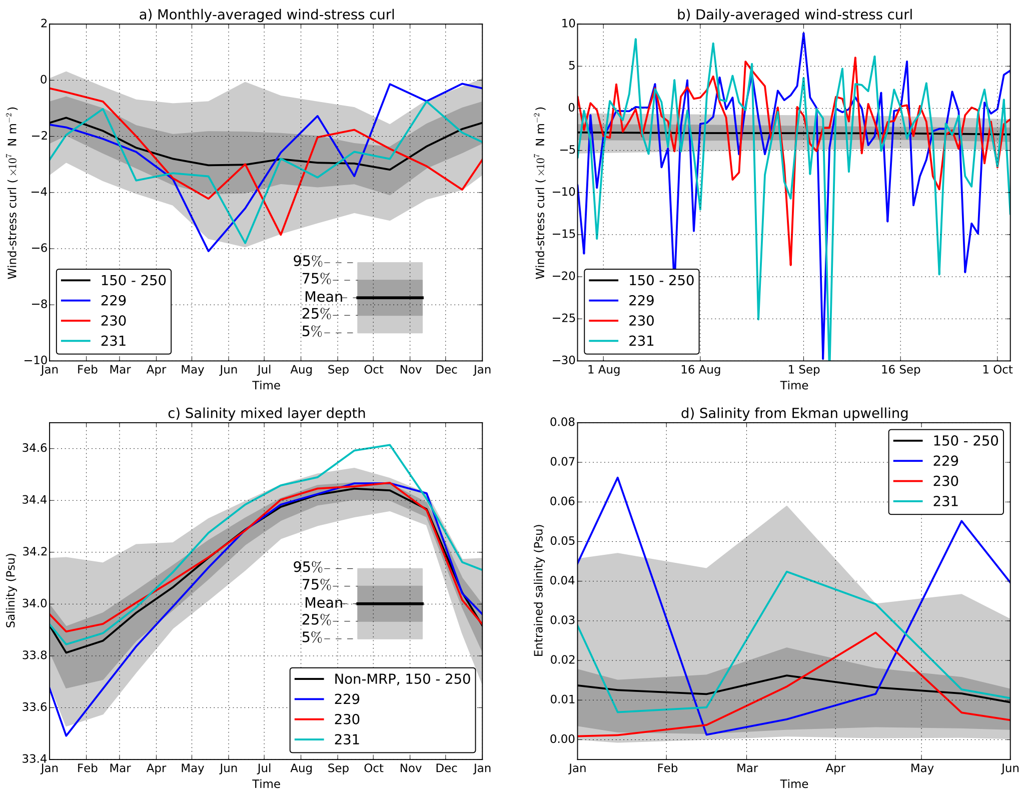

Figure 2: (a): Monthly-averaged magnitude of the wind-stress curl over the Polynya region for model years 229, 230 and 231. The shading indicates the climate variability, where the dark (light) shading correspond to the 25% – 75% (5% – 95%) percentile levels, the black curve is the climatology mean (model years 150 – 250). (b): Same as a), but now for daily averages. The shading is the same as in a). (c): Depth-averaged salinity over the mixed layer depth for model years 229, 230 and 231. The shading indicates the climate variability of this quantity (same as a)), but now only the non-MRP years are considered in the climatology. (d): The entrained salinity into the mixed layer from Ekman dynamics for model year 229, 230 and 231. The shading indicates the climate variability of this quantity (same as a)).

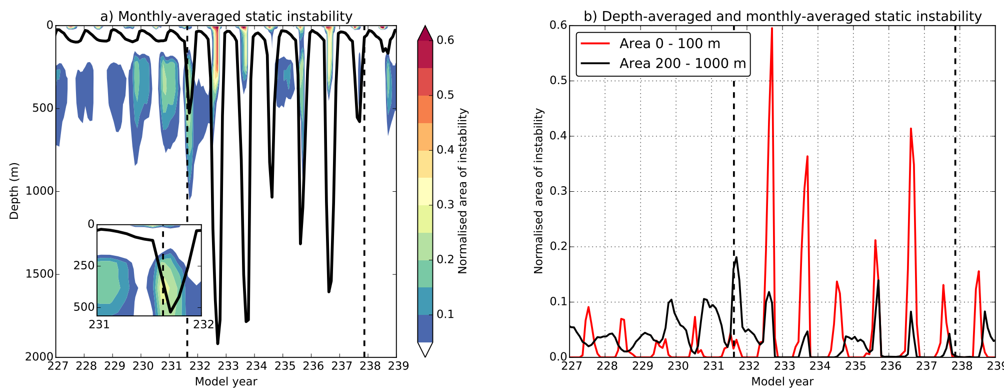

Figure 3: (a): Area per depth level where the water column in the Polynya region is statically unstable ($\mathcal{S} > 0$), normalised to the total area at that depth level. (b): The depth-averaged normalised area of static instabilities over the upper 100 m and between 200 – 1000 m. In both figures, the dashed lines indicate the beginning (model year 231) and ending (model year 237) of the multiyear MRPs. The model output analysed consists of monthly averages.

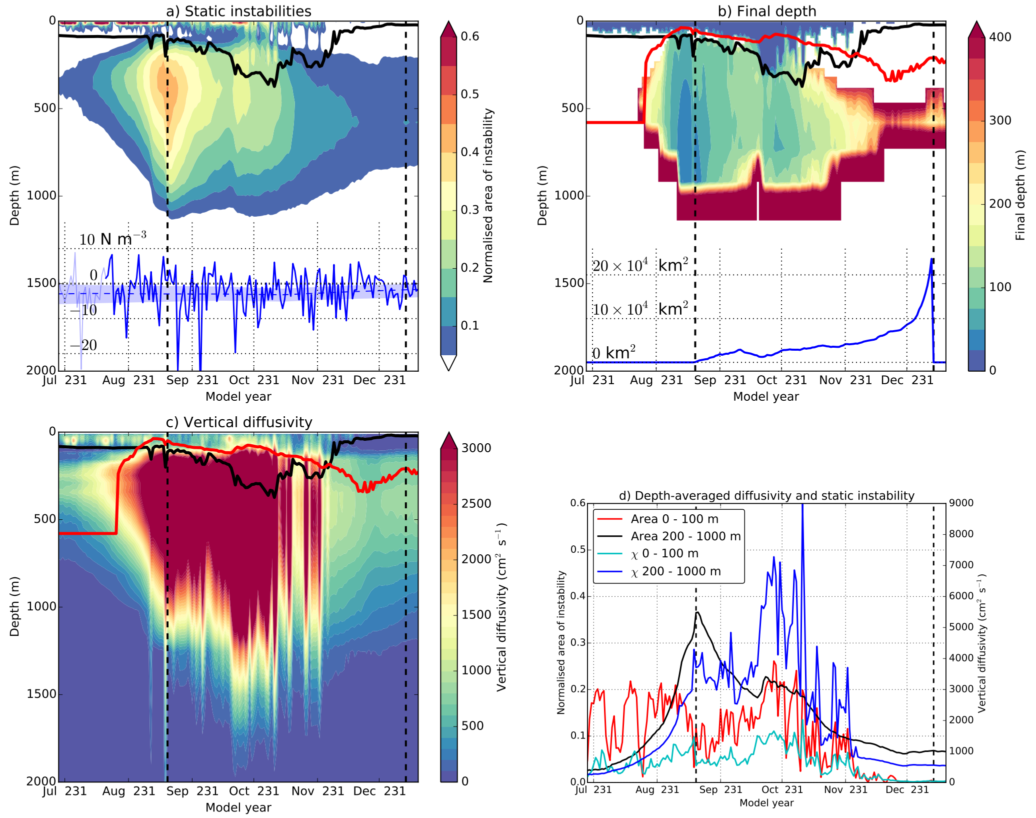

Figure 4: (a): Area per depth level where the water column in the Polynya region is statically unstable ($\mathcal{S} > 0$), normalised to the total area at that depth level. The blue curve is the daily-averaged magnitude of the wind-stress curl over the Polynya region, same as in Figure 2b. (b): Final depth of fluid elements due to (subsurface) convection. Only regions where deviations from the initial depth occur are displayed. The red curve shows the final depth of convection initially starting at $z_{ref} = 580$ m. The blue curve (bottom part) is the total area of the model year 231 MRP. (c): The vertical diffusivity (χ) for temperature, spatially averaged over the Polynya region. The red curve is the same as in b). In a) – c), the black curve shows the maximum mixed layer depth spatially averaged over the Polynya region. (d): The depth-averaged vertical diffusivity (χ) and normalised area of static instabilities over the upper 100 m and between 200 – 1000 m. In all figures, the dashed lines indicate the formation (20 August) and ending (14 December) of the MRP.